Kovove Mater. 49 2011 119–124
DOI: 10.4149/km_2011_2_119

Hardness and indentation load-size effect in Al_2O_3-SiC nanocomposites

E. Csehová[1], J. Andrejovská[1]*, A. Limpichaipanit[2], J. Dusza[1], R. Todd[2]

[1] *Institute of Materials Research, Slovak Academy of Sciences, Watsonova 47, 040 01 Košice, Slovak Republic*
[2] *Department of Materials, University of Oxford, Parks Road, Oxford OX1 3PH, United Kingdom*

Received 24 February 2010, received in revised form 19 October 2010, accepted 16 November 2010

Abstract

The indentation load-size effect (ISE) in Vickers hardness of Al_2O_3 and Al_2O_3 + SiC nanocomposites has been investigated using Meyer's law, the proportional specimen resistance (PSR) model and the modified proportional specimen resistance (MPSR) model. The strongest ISE was found for alumina. It is suggested that the smaller ISE in the nanocomposites is associated with the large thermal residual stresses and pre-existing dislocations in these materials, both of which would help the initiation of plastic deformation. Both the PSR and MPSR models described the ISE well, but the MPSR model resulted in slightly lower true hardness values for all materials investigated. There was no evidence of an effect of machining stresses on the ISE.

K e y w o r d s: nanocomposites, hardness, microstructure, residual stresses

1. Introduction

After the presentation of the new design concept of ceramic nanocomposites by Niihara and co-workers [1], intensive research started all over the world with the aim of improving the mechanical properties of different ceramic materials, e.g. [1–10]. Niihara et al. reported a significant increase in room and high temperature mechanical properties of ceramic nanocomposites, e.g. Al_2O_3 + SiC, however, the majority of recent investigations show that the dispersion of SiC nanoparticles in an alumina matrix results in higher hardness and wear resistance but only in a moderate strength improvement and in ambiguous results as regards the fracture toughness [4–7].

It has frequently been reported that the apparent hardness of a given ceramic material is a function of the applied testing load; the measured hardness increases with decreasing load [11, 12]. To explain this so called "indentation load/size effect – ISE" intensive research has been performed during the last decade, based on which different explanations have been advanced. According to Bückle the ISE is directly related to intrinsic structural factors of the test materials. Others reported that dislocation and twin activity or the formation of cracks may cause the ISE [13, 14].

Several empirical or semi-empirical equations, including Meyer's law [15], the Hays-Kendall approach [16], the energy-balance approach [17, 18], the proportional specimen resistance (PSR) model [12], etc. have been proposed for describing the variation of the indentation hardness with the applied indentation load. Probably the most widely used empirical equation for describing the ISE is Meyer's law, which gives an expression relating the load P and the size of indentation d of the form:

$$P = A \cdot d^n, \tag{1}$$

where the exponent n, i.e. Meyer's index, is the measure of the ISE, and A is a constant.

Li and Bradt in their PSR model [12], prepared on the basis of the work in [16], suggested that the specimen resistance, W, during indentation is not a constant, as was proposed by Hays and Kendall, but increases with the indentation size and is directly proportional to it according to the relationship:

*Corresponding author: tel.: +421 55 7922 457; fax: +421 55 7922 4408; e-mail address: jandrejovska@imr.saske.sk

$$W = a_1 d \tag{2}$$

and the effective indentation load and the indentation dimension are therefore related as follows:

$$P_{\text{eff}} = P - W = P - a_1 d = a_2 d^2, \tag{3}$$

where the parameters a_1 and a_2 can be related to the elastic and plastic properties of the tested material, respectively.

Gong et al. [19] suggested a modified PSR model based on the consideration of the effect of the machining-induced residual stresses at the surface during the indentation in the form

$$P = P_0 + a_1 d + a_2 d^2, \tag{4}$$

where P_0 – residual stress in the material – is a constant and a_1 and a_2 are the same parameters as in the PSR model.

The investigations up to now concerning the ISE in ceramics have focused mainly on single crystals, monolithic and composite ceramics and only a limited investigation has been carried out on ceramic nanocomposites, which are interesting to investigate in this respect because of the very large residual stresses within them originating from the different thermal expansion coefficient of the constituent phases.

The aim of the present investigation is therefore to study the load dependence of the measured Vickers hardness of alumina-silicon carbide micro/nanocomposites and to examine the indentation-size effect using different models. The results provide new information on the response of nanocomposites to indentation and help to clarify the microstructural factors contributing to the ISE by comparing materials with the same alumina matrix, but with the clear differences defined by the presence or absence of SiC nanoparticulate inclusions.

2. Experimental materials and methods

Alumina (Al_2O_3) and Al_2O_3-SiC nanocomposites with 5 vol.% (A5%SiC) and 10 vol.% (A10%SiC) of SiC particles were prepared from fine α-alumina (Sumitomo AKP50, Japan, mean particle size 200 nm) and SiC (Lonza UF45, Germany, mean particle size 260 nm) + 0.25 wt.% MgO to prevent abnormal grain growth, following an aqueous route described previously [9, 10]. The powders were mixed with distilled water (4 : 1 water to powder by volume) and a dispersant (Dispex A40, Ciba, Bradford, UK) and the slurry was attrition milled (Szegvari HD-01, USA) using YSZ milling media and freeze dried (Edwards Micromodulyo, UK). The dried powder was passed through a 150 µm sieve and calcined at 600 ℃ in air for 1 h to remove the dispersant. Discs were hot pressed in a graphite die for 30 min at 25 MPa in an argon atmosphere at 1700 ℃ for the nanocomposites and 1550 ℃ for the pure alumina in order to obtain specimens with similar grain sizes.

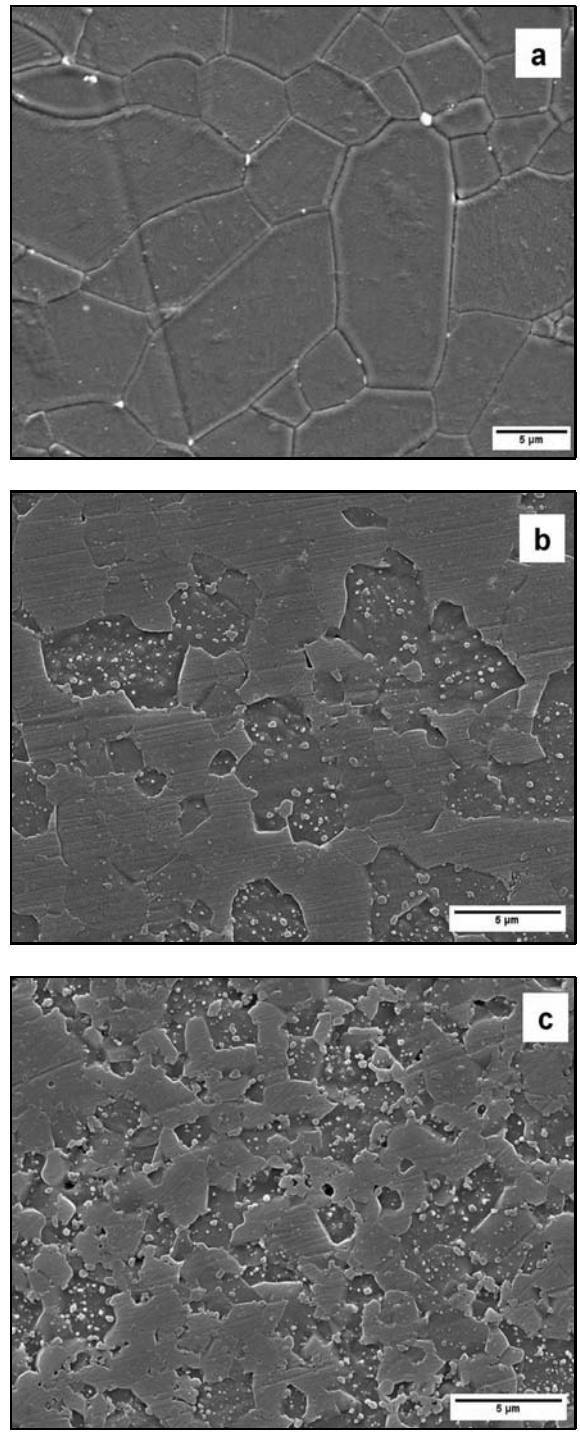

Fig. 1. Characteristic microstructure of the monolithic alumina (a) and the nanocomposites with 5 vol.% (b) and 10 vol.% (c) SiC, chemically etched, SEM.

The resulting dense (> 99 %) specimens were cut

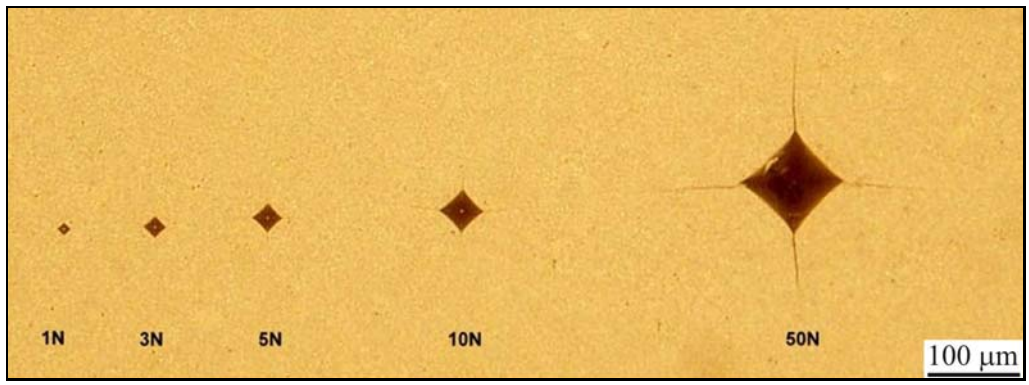

Fig. 2. Indents in the composite with 5 vol.% of SiC, SEM.

and polished using diamond paste to a 1 μm finish, and chemically etched for 5 min in 85 % concentrated H_3PO_4 at 230 ℃.

The size of the alumina matrix grains and the SiC particles were quantified by standard image analysis (software Image J) of the micrographs.

The microstructure of the obtained specimens was observed by scanning electron microscopy (JEOL JSM-7000F). Specimen surfaces were coated with gold in order to eliminate charging effects under electron irradiation.

The hardness of the specimens was measured by Vickers diamond indenter with applied loads ranging from 1 N to 49.05 N for 10 s using an HV-50A Hardness tester and Micro hardness Tester LECO LM-700AT. The Vickers hardness was calculated by Eq. (5):

$$\mathrm{HV} = \frac{1.8544 \times P}{d^2}, \tag{5}$$

where HV is the Vickers hardness, P is the indentation load, and d is the average diagonal length of the indents. At least ten indents were measured and used for the hardness calculation for each material and indentation load.

The parameters of Meyer's law (Eq. 1), n and A, have been derived directly from straight line fitting of the experimental data in the relationship $\log d$ vs. $\log P$. According to Eqs. (1) and (2), if $n < 2$, there is an ISE on hardness and when $n = 2$, the hardness is independent of the applied load.

The coefficients of the proportional specimen resistance (PSR), a_1 and a_2, were evaluated through the linear regression of P/d versus d (see Eq. (3)). Similarly, the parameters of the modified PSR were obtained by conventional polynomial regression of the plot P vs. d, according to Eq. (4).

3. Results and discussion

Characteristic microstructures of monolithic alumina and alumina based composites are illustrated in Fig. 1. According to the microstructure analysis the alumina grains in the monolithic material and in the composites with 5 vol.% and 10 vol.% of SiC additives were in the interval from 3.4–3.9 μm, 1.9–2.2 μm and 1.5–1.9 μm, respectively. The SiC nanoparticles in the composites were distributed predominantly intragranularly within the alumina grains. The size of the SiC grains in the A5%SiC composite ranged from 100 to 260 nm and in the A10%SiC composite from 60 to 130 nm, possibly because the higher SiC content in the latter made milling more efficient [20]. A small number of processing flaws in the form of pores or clusters of SiC grains could be identified.

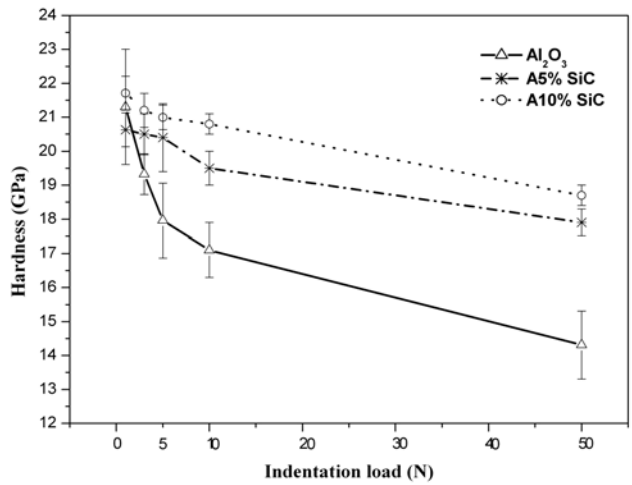

Fig. 3. Influence of the indentation load on the Vickers hardness of the investigated materials.

As shown in Fig. 2, the indentation cracks were formed in all indents at all indentation loads in the range from 1 N to 50 N. However, no indentation cracks were observed when the lowest load had been applied. Such cracks are helpful for estimation of the fracture toughness of the investigated ceramics, but they can influence the true hardness values [21, 22].

In Fig. 3, the influence of the indentation load on the hardness of Al_2O_3 and the composites is illus-

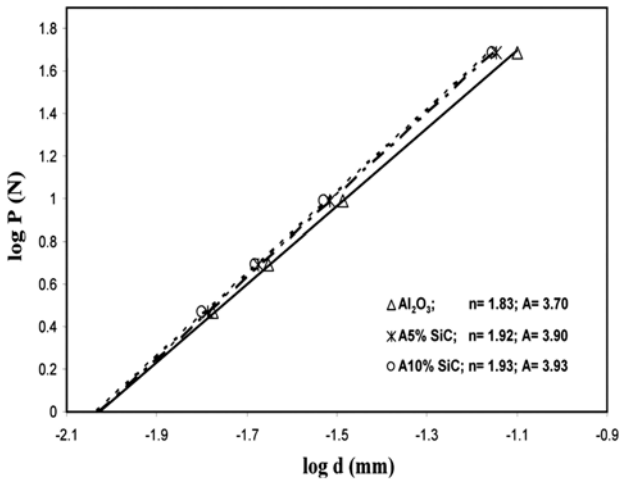

Fig. 4. Dependence of log$P$ on log$d$ according to Meyer's law for tested materials.

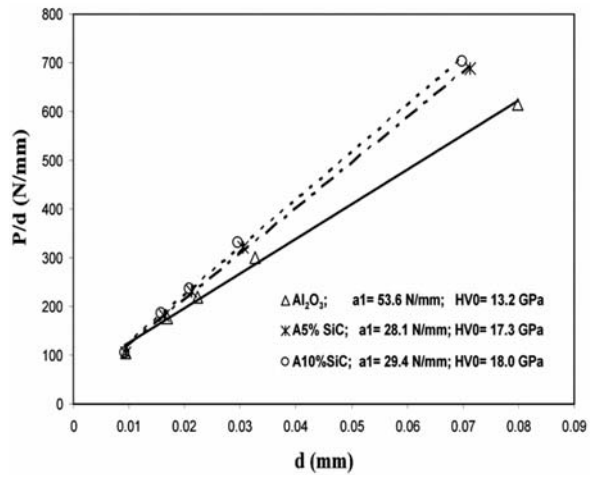

Fig. 5. Dependence of P/d on d according to the PSR model for tested materials.

trated. According to the results for all investigated materials the hardness increased with decreasing indentation load and with increasing volume fraction of SiC. The lowest hardness was found for the alumina but with decreasing load its hardness increased faster in comparison to those of the composites, and at the lowest indentation load the hardness values of all materials were very similar. The highest scatter was found in the case of alumina and the scatter for all materials seems to be approximately constant for all applied loads.

The load-dependence of the Vickers hardness can be described quantitatively by Meyer's law, Eq. (1). Figure 4 illustrates the Meyer's law parameters determined by the regression analyses of the results. According to the results, the most significant ISE was found in alumina ($n = 1.83$) and the ISE observed in the composites ($n = 1.92$ and $n = 1.93$) was much less pronounced. These values lie within the range for n of 1.748 to 1.979 obtained for a variety of ceramics and glasses with indentation loads from 5 to 50 N by Gong et al. [19]. Like Gong et al., we found radial cracking at the corners of the indents for tested materials in the range of applied loads from 5 N to 50 N. Gong et al. pointed out that this may affect the hardness values obtained but since it is difficult to suppress this cracking, the extent of its influence on hardness is not clear [19].

It seems to be impossible to avoid the effect of microstructure on the hardness values in the low-load range, in which the ISE is significant. In the case of these materials, for a Vickers indentation with a load of 10 N the indent area is approximately 600 μm^2, including approximately 100 grains, which is sufficient for the characteristic of the material as a whole. With decreasing indentation load the indent size decreased and the indentation may then be able to sample regions with locally different microstructures, e.g. alumina grains with less or more than the average content of SiC nanoparticles, or alumina grains with different orientations, which will influence the resulting hardness significantly. The evidence here is that the nanocomposites showed smaller scatter in hardness than pure alumina which indicates that inhomogeneities in particle distribution do not significantly affect the hardness. The better defined hardness in the nanocomposites may be a consequence of the suppression of surface microcracking in these materials by the SiC particles within the alumina grains [9, 10]. The smaller scatter of measured hardness values in nanocomposites (mainly at low loads) can be explained by their fine grained microstructure, too.

Figure 5 shows the plot of P/d versus d for the materials investigated, with the slope of the straight lines of a_2 and an intercept equal to a_1 (see Eq. (3)). The correlation for all plots is high although a slight systematic curvature is evident with the same sense in all three materials. According to Li and Bradt [12] who investigated the microhardness indentation load size effect in TiO_2 and SnO_2 single crystals, if the fact that the power-law exponent, $n < 2$, is the result of not taking the proportional specimen resistance of the test specimen into account, then there must exist an inverse correlation between n and the a_1 values that describe the PSR model. An inverse correlation exists in our results between the n and a_1 values for the alumina and the nanocomposites, and extrapolating linearly to $a_1 = 0$ gives a value for n of 2.02, close to the ideal value of 2 required mathematically by a comparison of Eqs. (1) and (3) for materials with similar underlying hardness. This shows that both Meyer's law and the PSR model give reasonable mathematical fits to data exhibiting an ISE but there is nothing in this analysis supporting any particular physical interpret-

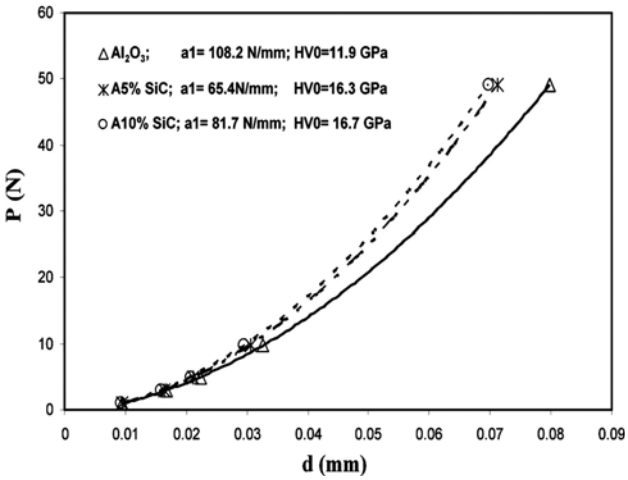

Fig. 6. Dependence of P on d for tested materials according to the MPSR model.

ation. The values for a_1 shown in Fig. 5 are significantly smaller for the nanocomposites than for the alumina, indicating according to the physical rationalisation of the PSR model a lower "specimen resistance" to indentation in the nanocomposites. One reason for this may be that the large, deviatoric thermal residual stresses in the nanocomposites help to initiate plastic deformation under low indentation loads. Using the Selsing formula [23] and the physical properties (as the coefficient of thermal expansion, modulus of elasticity and Poisson's ratio) of the matrix (m) and particle (p), $\alpha_m = 8.8 \times 10^{-6}\,K^{-1}$, $E_m = 380\,GPa$, $\nu_m = 0.21$ and $\alpha_p = 4.7 \times 10^{-6}\,K^{-1}$, $E_p = 490\,GPa$, $\nu_p = 0.19$, the matrix residual stresses close to the particles can be calculated to be approximately $\sigma = -2\,GPa$ in the radial direction and $+1\,GPa$ in the tangential direction. Stresses of this magnitude have also been confirmed experimentally [24–26]. A further reason for the ease of initiation of plastic deformation in the nanocomposites may be that the alumina grains of the nanocomposites are observed to contain many dislocations [1] even in the as processed condition, so there is no need to nucleate new dislocations in the early stages of indentation.

The term a_2 in the linear fits in Fig. 5 describes the load independent, so called "true hardness", which was found for Al_2O_3, A5%SiC and A10%SiC to be 13.2 GPa, 17.3 GPa and 18.0 GPa, respectively.

Gong et al. [19] investigated the ISE in ceramics with fracture toughness from 0.8 MPa $m^{0.5}$ to 12.4 MPa $m^{0.5}$. They found that for some ceramics the PSR model did not provide a satisfactory explanation of the ISE and offered a modified PSR model to solve this problem, see Eq. (4). The term P_0 in this model was rationalised by Gong et al. in relation to the residual surface stresses in the test specimen associated with the machining and polishing of the samples prior to testing. In Fig. 6, the relationship between P and the indentation size d is illustrated in the form of polynomial curves with the calculated parameters of the modified PSR model. The correlation is very good, although the introduction of an extra adjustable parameter (P_0) is bound to lead to improved fitting, whatever the correct physical explanation of the ISE. In the present case, the values of P_0 were negative for the monolithic alumina and for the composites too, as was found by Gong et al. [19], with values of –0.67, –0.43 and –0.60 N for the Al_2O_3, A5%SiC and A10%SiC, respectively. Therefore, there is no systematic trend apparent that may relate to microstructure or surface residual stresses from machining. If anything, these machining stresses would be expected to be greater in the nanocomposites [25], but it seems unlikely that they could have influenced the current results significantly since relatively high loads have been used and the machining stresses after polishing are confined to a very thin surface layer [28]. The lack of any systematic difference between the alumina and the nanocomposites also suggests that P_0 is not related to thermal residual stresses.

The MPSR model results in slightly lower "true hardness" values of 11.9, 16.3 and 16.7 GPa, for the Al_2O_3, A5%SiC and A10%SiC ceramics, respectively, although the trend in hardness with SiC addition is the same as was found for the PSR.

Recently Curkovic et al. [29] found the indentation size effect in slip-casted high purity alumina during Vickers hardness test in the load range from 0.5 N to 50 N. They found the best correlation between the measured values and the mathematical model in the case of MPSR model, however, in their investigation the P_0 value was positive, approximately 0.18 N.

The ISE of different ceramics has recently been investigated using nanoindentation data measured in the peak-load range from 7.5 to 500 mN by Peng et al. [30]. The results were analysed using several models, including those considered here, and the authors concluded that both Meyer's law and the MPSR model gave good descriptions of the ISE, but that a clear relationship to physical meaning was difficult to establish. They found very similar but high (e.g. for Si_3N_4 equal to approximately 19 GPa) true hardness values using the different models. The different values of true hardness obtained by applying different models in our experiment is probably the result of the higher applied loads in comparison to the indentation loads in [30]. At such loads the influence of the residual stresses is probably not significant, therefore their influence at describing the ISE was not recognized. The influence of the residual stresses on the applicability of different models at lower indentation loads will be the subject of future investigation.

4. Conclusions

The load dependence of the measured Vickers hardness of monolithic alumina and alumina-silicon carbide micro/nanocomposites has been investigated and the ISE has been examined based on different models. The strongest ISE was found for alumina with Meyer's index of $n = 1.83$, and in the case of composites the ISE was significantly lower with Meyer's index $n = 1.93$ and $n = 1.92$. Both the PSR and modified PSR models have been found suitable for describing the ISE, however the modified PSR model results in lower true hardness values for all investigated materials. The lower ISE for the nanocomposites was attributed to the high thermal stresses and pre-existing dislocation distributions in these materials. No evidence was found for the influence of machining stresses on the ISE and it is likely that the introduction of P_0 in the modified PSR model improves the fit to results mainly by providing an extra adjustable variable rather corresponding to the simple physical phenomenon.

Acknowledgements

This work was partly supported by APVV LPP 0174--07, LPP-0203-07, APVV-0171-06, APVV-0034-07, COST--0042-06 and NANOSMART Centre of Excellence, SAS.

References

[1] NIIHARA, K.: J. Ceram. Soc. Jpn., *99*, 1991, p. 974.
[2] LIU, H.—HUANG, CH.: Mater. Science and Engineering, *487*, 2008, p. 258. doi:10.1016/j.msea.2007.10.072
[3] CARROLL, L.—STERNITZKE, M.—DERBY, B.: Acta Mater., *44*, 1996, p. 4543. doi:10.1016/1359-6454(96)00074-2
[4] ZHAO, J.—STEARNS, L. C.—HARMER, M. P.—CHAN, H. M.—MILLER, G. A.—COOK, R. F.: J. Am. Ceram. Soc., *76*, 1993, p. 503. doi:10.1111/j.1151-2916.1993.tb03814.x
[5] BORSA, C. E.—JIAO, S.—TODD, R. I.—BROOK, R. J.: J. Microsc., *177*, 1995, p. 305.
[6] PEZZOTTI, G.—SAKAI, M.: J. Am. Ceram. Soc., *77*, 1994, p. 3039. doi:10.1111/j.1151-2916.1994.tb04545.x
[7] GALUSEK, D.—SEDLÁČEK, J.: J. Eu. Ceram. Soc., *27*, 2007, p. 2385. doi:10.1016/j.jeurceramsoc.2006.09.007
[8] WALKER, C. N.—BORSA, C. E.—TODD, R. I.—DAVIDGE, R. W.—BROOK, R. J.: British Ceramic Proc., *53*, 1994, p. 249.
[9] ORTIZ MERINO, J. L.—TODD, R. I.: Acta Mater., *53*, 2005, p. 3345.
[10] LIMPICHAIPANIT, A.—TODD, R. I.: J. Eur. Ceram. Soc., *29*, 2009, p. 2841. doi:10.1016/j.jeurceramsoc.2009.03.023
[11] CLINTON, D. J.—MORELL, R.: Mater. Chem. Phys., *17*, 1987, p. 461. doi:10.1016/0254-0584(87)90096-4
[12] LI, H.—BRADT, R. C.: J. Mater. Sci., *28*, 1993, p. 917. doi:10.1007/BF00400874
[13] BÜCKLE, I. H.: Metall. Rev., *4*, 1959, p. 49.
[14] MASON, W.—JOHNSON, P. F.—VARNER, J. R.: J. Mater. Sci., *26*, 1991, p. 6576. doi:10.1007/BF02402648
[15] TABOR, D.: The Hardness of Metals. Oxford, UK, Oxford University Press 1951.
[16] HAYS, C.—KENDALL, E. G.: Metall., *6*, 1973, p. 275. doi:10.1016/0026-0800(73)90053-0
[17] FROEHLICH, F.—GRAU, P.—GRELLMANN, W.: Phys. Status Solidi, *42*, 1977, p. 79.
[18] QUINN, J. B.—QUINN, G. D.: J. Mater. Sci., *32*, 1997, p. 4331. doi:10.1023/A:1018671823059
[19] GONG, J.—WU, J.—GUAN, Z.: J. Eur. Ceram. Soc., *19*, 1999, p. 2625. doi:10.1016/S0955-2219(99)00043-6
[20] STERNITZKE, M.: J. Eur. Ceram. Soc., *17*, 1997, p. 1061. doi:10.1016/S0955-2219(96)00222-1
[21] ANSTIS, G. R.—CHANTIKUL, P.—LAWN, B. R.—MARSHALL, D. B.: J. Am. Ceram. Soc., *64*, 1981, p. 533. doi:10.1111/j.1151-2916.1981.tb10320.x
[22] GONDÁR, E.—ROŠKO, M.—ZEMÁNKOVÁ, M.: Kovove Mater., *46*, 2005, p. 124.
[23] SELSING, J.: J. Am. Ceram. Soc., *44*, 1961, p. 419. doi:10.1111/j.1151-2916.1961.tb15475.x
[24] LEVIN, I.—KAPLAN, W. D.—BRANDON, D. G.—WIEDER, T.: Acta Mater., *42*, 1994, p. 1147. doi:10.1016/0956-7151(94)90131-7
[25] TODD, R. I.—BOURKE, M. A. M.—BORSA, C. E.—BROOK, R. J.: Acta Mater., *45*, 1997, p. 1791. doi:10.1016/S1359-6454(96)00273-X
[26] ORTIZ MERINO, J. L.—TODD, R. I.: J. Eur. Ceram. Soc., *23*, 2003, p. 1779. doi:10.1016/S0955-2219(02)00446-6
[27] TANNER, B. K.—WU, H. Z.—ROBERTS, S. G.: App. Phys. Lett., *86*, 2005, p. 061909.
[28] WU, H. Z.—ROBERTS, S. G.—WINN, A. J.—DERBY, B.: MRS Proc., *581*, 2000, p. 303.
[29] CURKOVIC, L.—LALIC, M.—SOLIC, S.: Kovove Mater., *47*, 2009, p. 89.
[30] PENG, Z.—GONG, J.—MIAO, H.: J. Eur. Ceram. Soc., *24*, 2004, p. 2193. doi:10.1016/S0955-2219(03)00641-1